BioNanoScience (2023) 13:2159–2167
https://doi.org/10.1007/s12668-023-01200-3

Potentiality Combined Heterogeneous Catalyst of Fe/TiO_2-Ni for Biodiesel Production from Coconut Oil

Maulidiyah Maulidiyah[1] · Abdul Haris Watoni[1] · Irwan Irwan[2] · La Ode Agus Salim[3] · Zul Arham[4] · Muhammad Nurdin[1]

Accepted: 10 September 2023 / Published online: 21 September 2023

Abstract
The present work is focused on the development of a potential novel heterogeneous catalyst for biodiesel production. A novel catalyst based on TiO_2 modified of 3d elements such as Fe and Ni metal (Fe/TiO_2-Ni). A series of Fe/TiO_2-Ni nanocomposites was prepared using a sol-gel method and calcined at 500 °C. The catalyst's surface morphology, structural crystal, and molecular structure were examined using a scanning electron microscope (SEM), using X-ray diffraction (XRD), and Fourier transform infrared (FTIR) analysis. The mean particle size of the Fe/TiO_2-Ni nanocomposite was estimated to be 9.16 nm. The results of nanocomposite analysis represented that the distribution of Fe and Ni elements in the lattice of TiO_2 nanoparticles has been successfully synthesized. The GC-MS analysis indicated that the main component of methyl ester for coconut oil contains methyl laurate ($C_{13}H_{26}O_2$) at 51.38%, methyl octanoate ($C_9H_{18}O_2$) at 18.75%, methyl caprate ($C_{11}H_{22}O_2$) at 10.21, and methyl myristate ($C_{14}H_{28}O_2$) at 8.80%. A catalyst examination was conducted following ASTM standards for coconut oil biodiesel production and was discovered to be within standards. Therefore, a catalyst based on TiO_2 modified of 3d elements (such as Fe and Ni metal) became a promising candidate for biodiesel production in the future.

Keywords Biodiesel · Transesterification · Coconut oil · Fe/TiO_2-Ni · Heterogeneous catalyst

1 Introduction

Currently, the increasing energy demand, depleting fossil fuel reserves, and several environmental issues have search lead for a renewable, eco-friendly alternative resource [1–3]. Among sundry renewable energy, biodiesel was considered a promising energy solution to the energy problem. Moreover, biodiesel proposes several excesses compared with diesel fuel such as non-toxic, renewable, and biodegradable [4–6]. Biodiesel, also familiar as fatty acid methyl ester, is generated through the transesterification reaction of vegetable oil/animal fats with an alcohol (methanol/ethanol) in the existence of a catalyst support [7–9]. In this stage, the catalyst becomes a very crucial part of biodiesel production. The catalyst utilized in the transesterification process can be either homogeneous or heterogeneous [10–12].

Nowadays, heterogeneous catalysts are preferred and more considerably used for biodiesel production than homogeneous catalysts. This is due to several reasons such as the homogeneous catalyst's lower biodiesel yield, difficult separation, non-reusability, and can pollute the environment [13–15]. These deficiencies of homogeneous catalysts could be overcome using heterogeneous catalysts because the catalysts could be recovered, easy to separate, environmentally friendly, as well as recycled [16–18]. Several heterogeneous catalysts that have been widely reported for biodiesel production include carbon-based [19], agricultural wastes [20], graphene-based metal oxide

✉ Muhammad Nurdin
mnurdin06@yahoo.com

1 Department of Chemistry, Faculty of Mathematics and Natural Sciences, Universitas Halu Oleo, Jl. H.E.A. Mokodompit Kampus Baru Anduonohu, Kendari, Southeast Sulawesi 93232, Indonesia

2 Department of Pharmacy, Faculty of Sciences and Technology, Institut Teknologi dan Kesehatan Avicenna, Kendari, Southeast Sulawesi 93117, Indonesia

3 Department of Chemistry, Faculty of Science and Technology, Institut Sains Teknologi dan Kesehatan (ISTEK) 'Aisyiyah Kendari, Kendari, Southeast Sulawesi 93116, Indonesia

4 Department of Mathematics and Natural Sciences, Institute Agama Islam Negeri (IAIN), Kendari, Southeast Sulawesi 93563, Indonesia

[21], modified resin [22], rare-earth metal [23], and shell waste [24]. Among the most examined heterogeneous catalyst, transition metal oxides such as titanium dioxide (TiO_2) have unique advantages in biodiesel production due to their higher basicity, easier to obtain, and inexpensive.

TiO_2 is one of the superior transition metal oxides that can be applied for biodiesel production as it is non-toxic and eco-friendly [25–29]. However, undoped TiO_2 has various limitations in its wide application. Furthermore, the selection of dopants also greatly affects the performance of TiO_2. Doping with 3d elements such as Fe and Ni metal can enhance the surface area, reduce the bandgap, increase the catalytic activity, and also reduce the particle size. The choice of Fe metal is caused by its stability at high temperatures, multivalent, and effectively reduces the band gap energy [30, 31]. Moreover, Fe metal is a magnetic oxide owning the ability to transesterify free fatty acid to achieve biodiesel products. The presence of Ni metal is also expected to increase the efficiency of TiO_2 photocatalysts in the visible region [32–34]. In addition to creating a new band gap, Ni doping can also accelerate photocatalytic activity and improve the transesterification process for biodiesel production [35]. The catalyst was synthesized by the sol-gel method and its catalytic performance was studied. At present, there are no studies reported that combined co-doped TiO_2 using 3d elements (Fe and Ni metal).

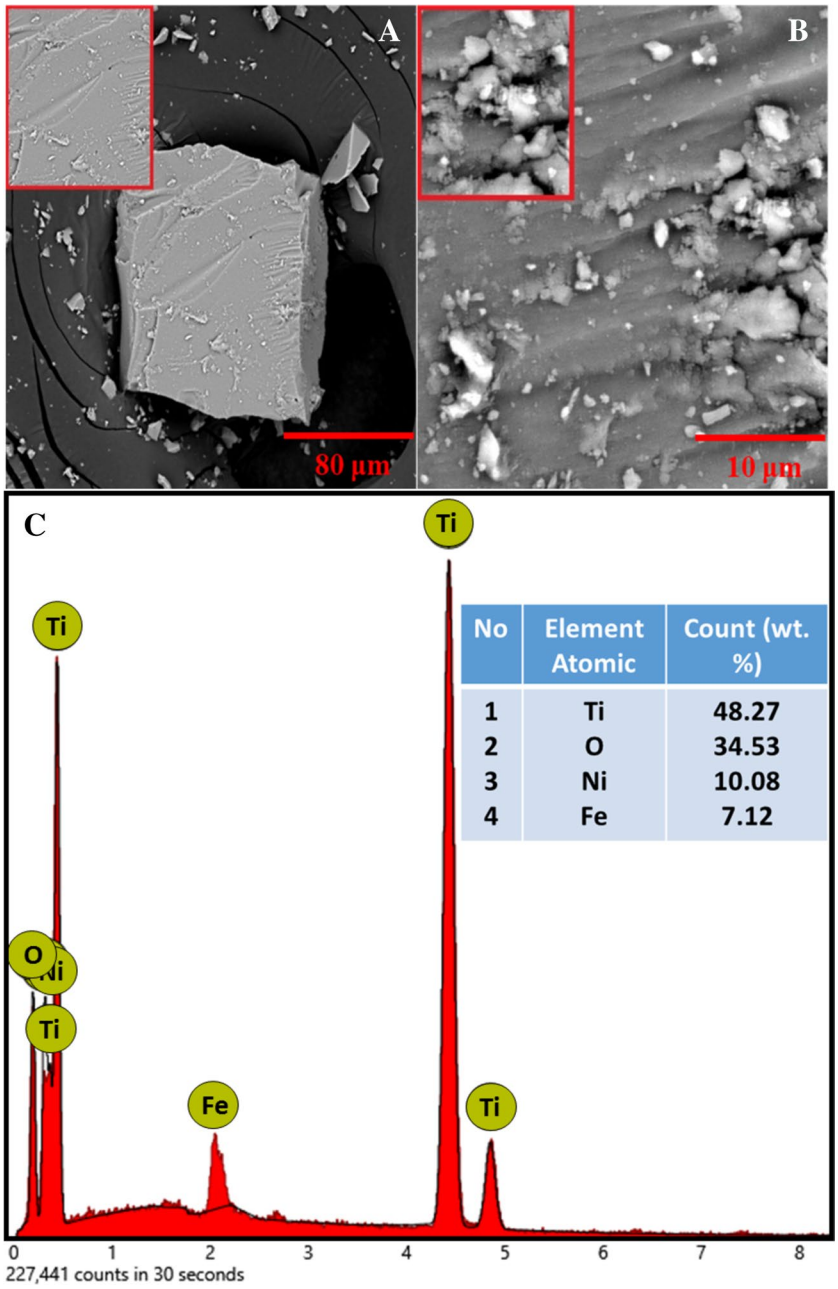

Fig. 1 SEM image of Fe/TiO_2-Ni nanocomposite (**a**) 1000 times, (**b**) 7500 times magnifications, and (**c**) EDX spectra of Fe/TiO_2-Ni

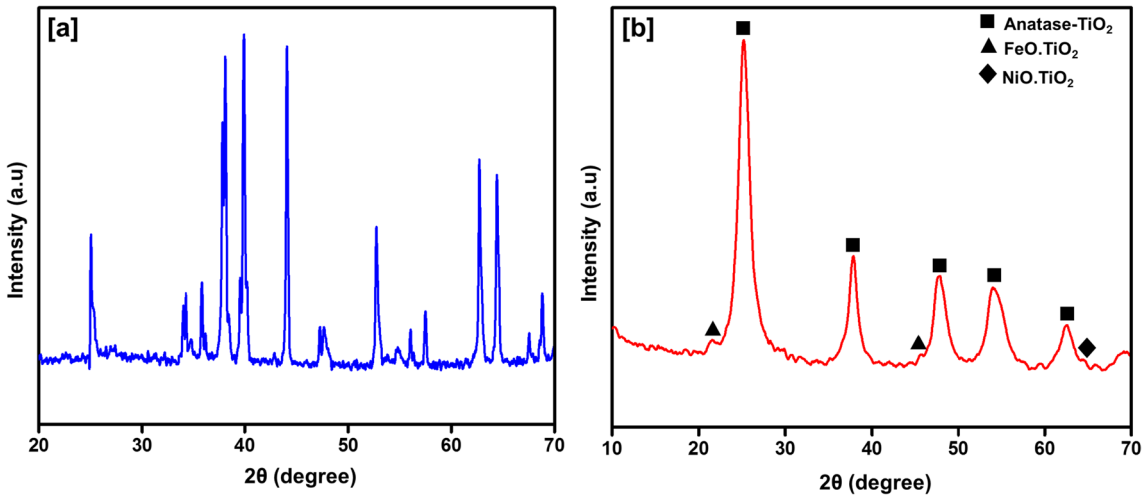

Fig. 2 XRD pattern of the (**a**) TiO_2 pure and (**b**) Fe/TiO_2-Ni catalyst

In the present work, we investigated Fe/TiO_2–Ni mixed nanocomposite as a heterogeneous catalyst for transesterification reaction that was efficiently utilized in biodiesel production from coconut oil. We also evaluated the effect of co-doped Fe and Ni against catalyst performance. Scanning electron microscopy (SEM), X-ray diffraction (XRD), Fourier transform infrared (FTIR) spectroscopy, scanning electron microscopy-energy dispersive X-ray (SEM-EDX), and gas chromatography and mass spectroscopy (GCMS) were conducted for the characterization of prepared catalysts and biodiesel product.

2 Materials and Method

2.1 Materials

The materials used in the present study were sodium hydroxide (NaOH) 0.1 N, ethanol (C_2H_5OH), iron(III) nitrate ($Fe(NO_3)_3$) 0.1 M, nickel(II) nitrate ($Ni(NO_3)_2$) 0.1 M, sodium thiosulfate ($Na_2S_2O_3$), titanium tetraisopropoxide (TTIP), iodide solution (I_2), chloroform ($CHCl_3$), acetyl acetonate ($C_5H_8O_2$), methanol (CH_3OH), distilled water, sulfate acid (H_2SO_4) (97 %), acetic acid (CH_3COOH) 0.5 M, phenolphthalein (PP) indicator, starch

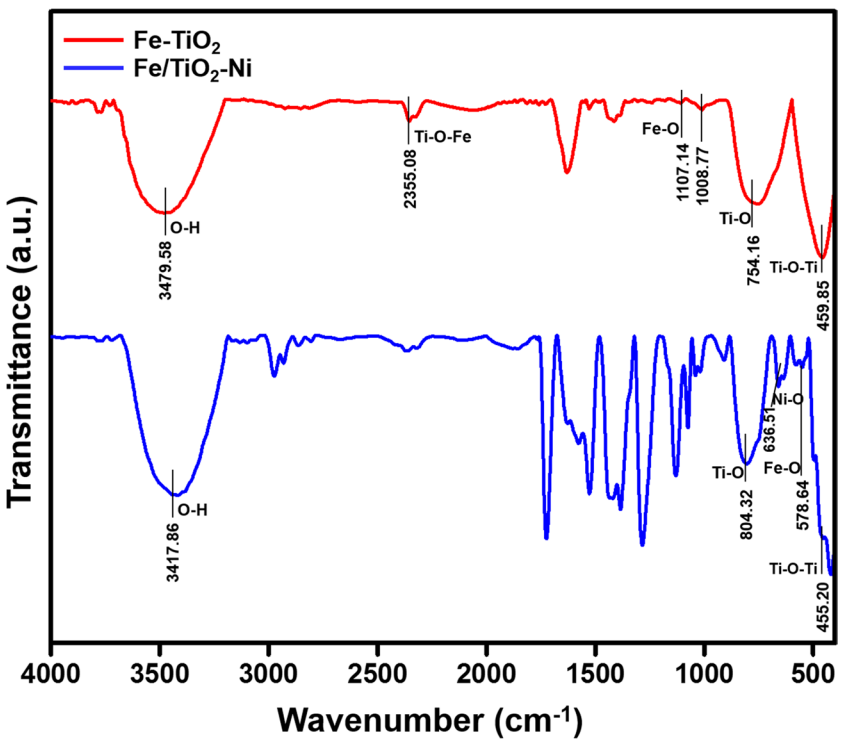

Fig. 3 FTIR spectra of (**a**) Fe-TiO_2 and (**b**) Fe/TiO_2-Ni

indicator, and n-hexane (C_6H_{14}). The coconut oil was pretreated by separating the meat from the shell. Furthermore, the meat was grated and squeezed to get coconut milk. The coconut milk was silenced to remove the water content. After pretreatment, the coconut milk was heated at 45 °C and for 5 h with vigorous stirring. After heating was completed, the coconut milk was cooled and filtered to achieve oil.

2.2 Catalyst Preparation

Fe/TiO_2-Ni nanocomposite was synthesized by the sol-gel method adapted from previous research: 4 mL of titanium tetraisopropoxide, 0.5 mL of acetyl acetonate, and 15 mL of ethanol were put into a beaker glass as solution A. Solution B was prepared by mixing 15 mL of ethanol, 2 mL distillate water, and 0.5 mL acetate acid. Furthermore, solutions A and B were refluxed for 3 h at 50 °C. Moreover, followed with added of 1 mL $Fe(NO_3)_3$ and $Ni(NO_3)_2$ 0.1 M and stirred using a magnetic stirrer for 1 h at 50 °C. Finally, the catalyst was calcined for 1 h at 400 °C.

2.3 Characterization

Fe/TiO_2-Ni nanocomposite was characterized using SEM-EDX analysis to observe the surface morphology, compositions, and also the micropore. Crystal shape and pore size were also observed using XRD analysis. The averaged diameter of the nanocomposite was determined using the Scherrer equation at 2θ between 10 and 80 °C. The crystal phases that exist in the samples were compared with the JCPDS database files. In addition, the structural composition and functional groups of the nanocomposite were also investigated using FTIR. FTIR studies for all the prepared samples were conducted in the 400–4000 cm^{-1} region.

2.4 Transesterification Reaction Studies

The transesterification reaction was conducted at the reactor system equipped with a hotplate stirrer and beaker assembled. The transesterification condition was diverse including the catalyst concentration (0.5, 1.0, and 1.5 b/v), oil:methanol mol ratio (1:6 mol: mol), reaction time (3 h), and under UV light. After the reaction was completed, the mixture was separated into the two-phase (biodiesel and glycerol) by using centrifugation for 5 min at 1600 rpm. The biodiesel obtained was placed in a bottle for methyl ester analysis. In the final stage, the methyl ester component was characterized using gas chromatography-mass spectroscopy.

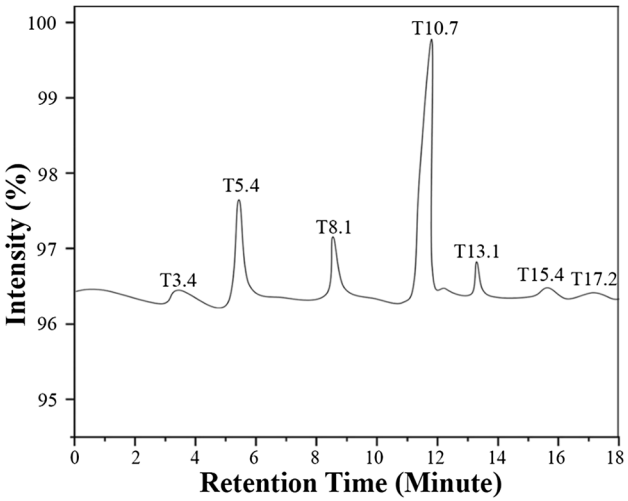

Fig. 4 Chromatogram of methyl ester

3 Results and Discussion

3.1 SEM-EDX Analysis

SEM images at different magnifications (1000 and 7500 times) of the Fe/TiO_2-Ni nanocomposite are displayed in Fig. 1. The preparation of the catalyst for the SEM analysis was conducted by the sol-gel method and calcined at 400°C for 1 h. SEM images (Fig. 1a) present the formation of agglomeration on the catalyst. The agglomeration suspectly originated from the calcination temperature and the existence of dopant ions distributed on the TiO_2 surface. Figure 1b illustrates the SEM images of the Fe/TiO_2-TiO_2 nanocomposite with magnification 7500 times. The catalyst exhibits TiO_2 nanoparticles on the surface material. TiO_2 particles are grainy in shape and irregular. In general, Fe/

Table 1 Composition of biodiesel conforming to the result of GC-MS analysis

Peak	R. time (min)	Compounds identified	Molecular formula	Composition (%)
1	3.44	Methyl caproate	$C_7H_{14}O_2$	1.44
2	5.49	Methyl octanoate	$C_9H_{18}O_2$	18.75
3	8.12	Methyl caprate	$C_{11}H_{22}O_2$	10.21
4	10.77	Methyl laurate	$C_{13}H_{26}O_2$	51.38
5	13.14	Methyl myristate	$C_{14}H_{28}O_2$	8.80
6	15.40	Methyl palmitate	$C_{17}H_{34}O_2$	2.02
7	17.19	Methyl oleate	$C_{19}H_{36}O_2$	1.44

TiO_2-Ni catalysts own an average size of 9.16 nm (colors of gray), suitable with Scherrer assessment. Therefore, the Fe/TiO_2-Ni nanocomposite could be classified as a heterogeneous catalyst reason the particles on a nano-size. The Fe/TiO_2-Ni composite also analyzed by EDX (Fig. 1c) indicates that it presents compositions such as Ti, O, Ni, and Fe elements. This result was supported by XRD and FTIR analyses and become an excuse for why the Fe/TiO_2-Ni catalyst showed the most excellent activity during the experiment.

3.2 XRD Analysis

The X-ray diffraction patterns of TiO_2 pure and Fe/TiO_2-Ni nanocomposite are shown in Fig. 2. Specifically, the pattern exhibits different peaks at 2θ of 21,43° and 45,69° was associated with the [101] and (004) fields of Fe-TiO_2 bond, correspond JCPDS No. 96-900-6336 [30]. The peaks at 2θ of 35,12° and 64,48° were associated with the [110] and [300] fields of the Ni-TiO_2 bond. These results are in accordance with the report by Gabal et al. [36]. Moreover, the peaks at 2θ of 25,24°; 37,79°; 47,48°; and 54,21°, 62,46°, and 69,70° are also visible and associated with the TiO_2 structure (JCPDS file no. 00-21-1272) with the crystal plane [101], [200], [004], [105], [211], and [220] [37]. The Fe/TiO_2-Ni nanocomposite crystalline size determined using Scherrer's equation was discovered approximately 9.16 nm.

3.3 FTIR Analysis

The FTIR spectrum of both Fe-TiO_2 and Fe/TiO_2-Ni nanocomposites is exhibited in Fig. 3. The wide band around 3417 cm^{-1} is associated with O–H group stretching and bending vibration, which is pertained to H_2O molecules. Moreover, the IR band is visible from 400 to 800 cm^{-1} according to the Ti–O stretching vibrations [38]. The absorption band at 636.51 cm^{-1}–659.66 cm^{-1}, typical for the Ni-O stretching vibration, ensures due to the presence of nickel oxide. The identical band at 600 cm^{-1}–700 cm^{-1} was also investigated by Ahmed et al. [39], which is shown that the (NO_3^-) group was always present when ($NaNO_3$) are utilized as precursor. Furthermore, the absorption band at 1039,62 cm^{-1} and 578,64 cm^{-1} was characterized as a vibration of Fe-O, which more convinces the existence of Fe in nanocomposite [40].

3.4 GC-MS Analysis

GC-MS analysis was determined to observe the presence of several kinds of fatty acid methyl ester from biodiesel products. The fatty acid methyl esters analysis characterized by GC-MS

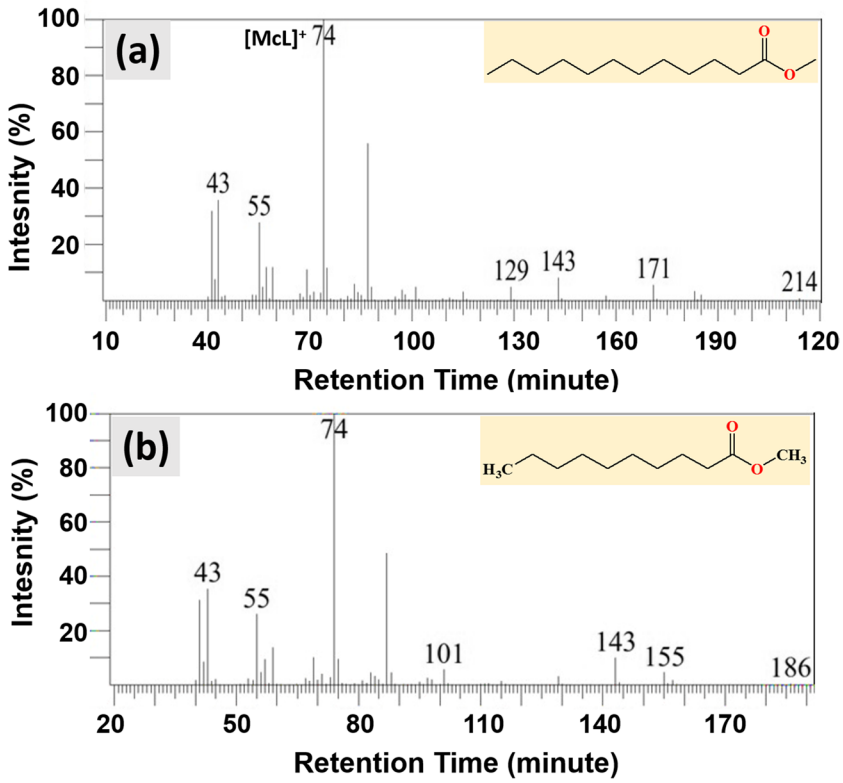

Fig. 5 GC-MS chromatogram of (**a**) methyl laurate and (**b**) methyl caprate

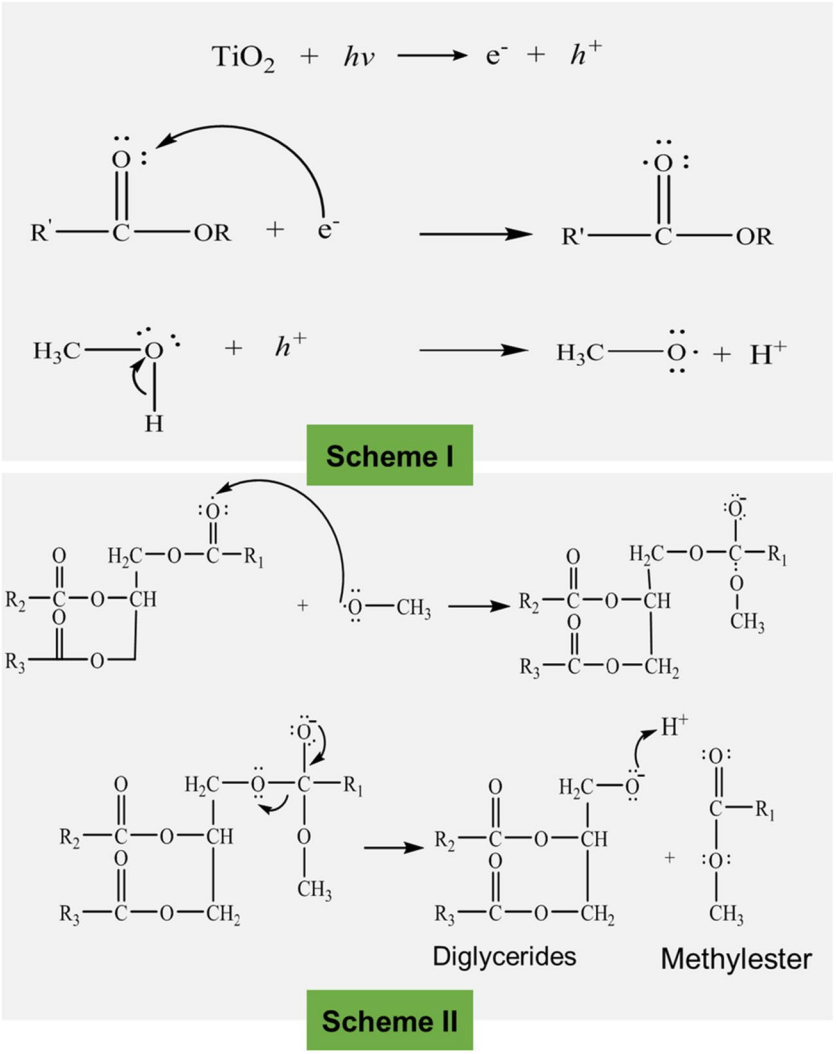

Fig. 6 The photocatalytic reaction mechanism using Fe/TiO_2-Ni heterogeneous catalyst in transesterification reaction

is displayed in Fig. 4 and visible in Table 1. The primary component discovers in biodiesel products such as methyl laurate ($C_{13}H_{26}O_2$), methyl octanoate ($C_9H_{18}O_2$), methyl caprate ($C_{11}H_{22}O_2$), and methyl myristate ($C_{14}H_{28}O_2$). The high peak at a retention time of 10.77 min in Fig. 4 and Table 1 presents the existence of methyl laurate with 51.38% of total content.

Figure 5a shows the primary peak in all the mass spectra of saturated methyl ester was observed at m/z 74 which is a rearrangement of McLafferty the well-known [41]. Three other peaks i.e., a peak at m/z 171, m/z 143, and m/z 129 due to the removal of a propyl radical (carbon 2 to 4). Moreover, methyl ester identified in coconut oil has characteristic fragmentation pattern peaks at m/z 55, $[M\text{-}]^+$ due to the removal of $C_3H_6O_2$. Figure 5b shows the mass spectrum of methyl caprate with a retention time of 8.127 min providing peaks with m/z of 43, 55, 74, and 101 respectively. Peaks at m/z 143 is due to the deletion of $C_8H_{15}O_2^+$. The other peaks at m/z 43, 101, and 143 are fragmentation patterns due to the

Table 2 Comparison of various feedstock in biodiesel production using heterogeneous catalysts

No.	Feedstock	Heterogeneous catalyst	Method	Reference
1	Canola oil	Li/TiO_2	Transesterification	[43]
2	Waste cooking oil	$S–TiO_2$/SBA-15	Esterification	[44]
3	Palm oil	Cu/TiO_2	Transesterification	[45]
4	Palm fatty acid	SO_3H-GO@TiO_2	Esterification	[46]
5	Coconut oil	Fe/TiO_2-Ni	Transesterification	In this work

cleavage of each C-C bond and are known as fragmentation patterns of the CnH_{2n}-$1O_2^+$ ion series [42].

The transesterification reaction using the Fe/TiO_2-Ni heterogeneous catalyst was performed in a UV reactor system. The mechanism of the Fe/TiO_2-Ni photocatalyst reaction was initiated with the process of transferring methanol and triglycerides to the surface of TiO_2. This process was accelerated through vigorous stirring. Methanol and triglycerides will be adsorbed on the surface of the photocatalyst. The proposed photocatalytic reaction mechanism can be seen in Fig. 6 (scheme 1). Based on Fig. 6 (scheme 1), electrons will react with triglycerides and produce RCO•OR radicals while holes react with methanol to form CH_3O• radicals. The two radicals produced will react to form methyl ester, as can be seen in Fig. 6 (scheme 2).

Moreover, numerous studies have previously documented a variety of comparisons involving the various feedstock in biodiesel production. These studies examined various heterogeneous catalysts, and their findings have been compiled and presented in Table 2.

4 Conclusions

The purpose of the present study was to increase the performance of TiO_2 in biodiesel production by adding 3d elements (such as Fe and Ni) using the sol-gel method and calcining at 500 °C. The surface morphology of nanocomposite depicted the grainy shape and irregular with an average size of 9.16 nm. The study indicated that the addition of 3d elements (Fe and Ni) has enhanced the TiO_2 surface area and activity against biodiesel production. GC-MS analysis of methyl ester for coconut oil revealed the existence of diverse compounds containing carbon atoms from C7 to C19. Its main components include methyl laurate (51.38%), methyl octanoate (18.75%), methyl caprate (10.21%), and methyl myristate (8.80%). On the whole, the TiO_2 modified of 3d elements (such as Fe and Ni) became a promising candidate as the heterogeneous catalyst for biodiesel production from coconut oil.

Author Contributions All authors contributed to the study conception and design. Material preparation, data collection, and analysis were performed by MM, AHW, and II. The first draft of the manuscript was written by LOAS, ZA, and MN and commented on previous versions of the manuscript. All authors read and approved the final manuscript.

Funding We acknowledge the financial support from the Ministry of Education, Culture, Research and Technology of the Republic of Indonesia under the Basic Research award grant no 65/UN29.20/PG/2022 and SP-DIPA-023.17.1.690523/2022 and thank the Universitas Halu Oleo for supporting this research.

Data Availability The datasets generated during and/or analyzed during the current study are available from the corresponding author on reasonable request.

Declarations

Research Involving Humans and Animals Statement This article does not contain any studies with human participants or animals performed by any of the authors.

Competing Interests The authors declare no competing interests.

References

1. Dahnum, D., Tasum, S. O., Triwahyuni, E., Nurdin, M., & Abimanyu, H. (2015). Comparison of SHF and SSF processes using enzyme and dry yeast for optimization of bioethanol production from empty fruit bunch. *Energy Procedia, 68*, 107–116.
2. Triwahyuni, E., Hariyanti, S., Dahnum, D., Nurdin, M., & Abimanyu, H. (2015). Optimization of saccharification and fermentation process in bioethanol production from oil palm fronds. *Procedia Chemistry, 16*, 141–148. https://doi.org/10.1016/j.proche.2015.12.002
3. Perumal, G., Rengasamy, T., & Dharmendira Kumar, M. (2017). Production of biodiesel by transesterification of Senna occidentalis nonedible oil. *Energy Sources, Part A: Recovery, Utilization, and Environmental Effects, 39*, 1855–1861.
4. Yaashikaa, P. R., Devi, M. K., Kumar, P. S., & Pandian, E. (2022). A review on biodiesel paroduction by algal biomass: Outlook on life-cycle assessment and techno-economic analysis. *Fuel, 324*, 124774.
5. M. Maulidiyah, A.H. Watoni, N. Maliana, I. Irwan, L.O.A. Salim, Z. Arham, M. Nurdin, Biodiesel production from crude palm oil using sulfuric acid and K2O catalysts through a two-stage reaction, (2021).
6. Chozhavendhan, S., Singh, M. V. P., Fransila, B., Kumar, R. P., & Devi, G. K. (2020). A review on influencing parameters of biodiesel production and purification processes. *Current Research in Green and Sustainable Chemistry, 1*, 1–6.
7. Günay, M. E., Türker, L., & Tapan, N. A. (2019). Significant parameters and technological advancements in biodiesel production systems. *Fuel, 250*, 27–41.
8. Patchimpet, J., Simpson, B. K., Sangkharak, K., & Klomklao, S. (2020). Optimization of process variables for the production of biodiesel by transesterification of used cooking oil using lipase from Nile tilapia viscera. *Renewable Energy, 153*, 861–869.
9. Govindhan, P., Prabhu, N. V., Edison Chandraseelan, R., & Dharmendira Kumar, M. (2022). Technologies of bio-diesel production: A state of the art review. *Petroleum Science and Technology*, 1–18.
10. Karthikeyan, M., Renganathan, S., & Govindhan, P. (2017). Production of biodiesel via two-step acid-base catalyzed transesterification reaction of Karanja oil by BaMoO4 as a catalyst. *Energy Sources, Part A: Recovery, Utilization, and Environmental Effects, 39*, 1504–1510.
11. Govindhan, P., Prabhu, N. V., Edison Chandraseelan, R., & Dharmendira Kumar, M. (2023). Green diesel production from Karanja oil using mesoporous Ba (HPW12O40) solid acid catalyst. *Petroleum Science and Technology, 41*, 1526–1545.
12. Perumal, G., & Mahendradas, D. K. (2022). Biodiesel production from Bauhinia variegata seeds oil using homogeneous catalyst. *Petroleum Science and Technology, 40*, 857–870.

13. Kamaronzaman, M. F. F., Kahar, H., Hassan, N., Hanafi, M. F., & Sapawe, N. (2020). Biodiesel production from waste cooking oil using nickel doped onto eggshell catalyst. *Materials Today: Proceedings, 31*, 342–346.
14. Sree, J. V., Chowdary, B. A., Kumar, K. S., Anbazhagan, M. P., & Subramanian, S. (2021). Optimization of the biodiesel production from waste cooking oil using homogeneous catalyst and heterogeneous catalysts. *Materials Today: Proceedings, 46*, 4900–4908.
15. Mukhtar, A., Saqib, S., Lin, H., Shah, M. U. H., Ullah, S., Younas, M., Rezakazemi, M., Ibrahim, M., Mahmood, A., & Asif, S. (2022). Current status and challenges in the heterogeneous catalysis for biodiesel production. *Renewable and Sustainable Energy Reviews, 157*, 112012.
16. Degfie, T. A., Mamo, T. T., & Mekonnen, Y. S. (2019). Optimized biodiesel production from waste cooking oil (WCO) using calcium oxide (CaO) nano-catalyst. *Scientific Reports, 9*, 18982.
17. Mamo, T. T., & Mekonnen, Y. S. (2020). Microwave-assisted biodiesel production from microalgae, Scenedesmus species, using goat bone–made nano-catalyst. *Applied Biochemistry and Biotechnology, 190*, 1147–1162.
18. Erchamo, Y. S., Mamo, T. T., Workneh, G. A., & Mekonnen, Y. S. (2021). Improved biodiesel production from waste cooking oil with mixed methanol–ethanol using enhanced eggshell-derived CaO nano-catalyst. *Scientific Reports, 11*, 6708.
19. Roy, M., & Mohanty, K. (2021). Valorization of de-oiled microalgal biomass as a carbon-based heterogeneous catalyst for a sustainable biodiesel production. *Bioresource Technology, 337*, 125424.
20. Awogbemi, O., Von Kallon, D. V., & Aigbodion, V. S. (2021). Trends in the development and utilization of agricultural wastes as heterogeneous catalyst for biodiesel production. *Journal of the Energy Institute, 98*, 244–258.
21. Jume, B. H., Gabris, M. A., Nodeh, H. R., Rezania, S., & Cho, J. (2020). Biodiesel production from waste cooking oil using a novel heterogeneous catalyst based on graphene oxide doped metal oxide nanoparticles. *Renewable Energy, 162*, 2182–2189.
22. Ma, Y., Wang, Q., Sun, X., Wu, C., & Gao, Z. (2017). Kinetics studies of biodiesel production from waste cooking oil using FeCl3-modified resin as heterogeneous catalyst. *Renewable Energy, 107*, 522–530.
23. Rezania, S., Korrani, Z. S., Gabris, M. A., Cho, J., Yadav, K. K., Cabral-Pinto, M. M. S., Alam, J., Ahamed, M., & Nodeh, H. R. (2021). Lanthanum phosphate foam as novel heterogeneous nanocatalyst for biodiesel production from waste cooking oil. *Renewable Energy, 176*, 228–236.
24. Pandit, P. R., & Fulekar, M. H. (2017). Egg shell waste as heterogeneous nanocatalyst for biodiesel production: Optimized by response surface methodology. *Journal of Environmental Management, 198*, 319–329.
25. Zul, A., Muhammad, N., & Buchari, B. (2016). Photoelectrocatalysis performance of la2O3 doped TiO2/Ti electrode in degradation of rhodamine B organic compound. *International Journal of ChemTech Research, 9*, 113–130.
26. Nurdin, M., Maulidiyah, M., Muzakkar, M. Z., & Umar, A. A. (2019). High performance cypermethrin pesticide detection using anatase TiO2-carbon paste nanocomposites electrode. *Microchemical Journal, 145*, 756–761.
27. Nurdin, M., Agusu, L., Putra, A. A. M., Maulidiyah, M., Arham, Z., Wibowo, D., Muzakkar, M. Z., & Umar, A. A. (2019). Synthesis and electrochemical performance of graphene-TiO2-carbon paste nanocomposites electrode in phenol detection. *Journal of Physics and Chemistry of Solids, 131*, 104–110.
28. Maulidiyah, M., Azis, T., Lindayani, L., Wibowo, D., Salim, L. O. A., Aladin, A., & Nurdin, M. (2019). Sol-gel TiO_2/carbon paste electrode nanocomposites for electrochemical-assisted sensing of fipronil pesticide. *Journal of Electrochemical Science and Technology, 10*. https://doi.org/10.33961/jecst.2019.00178
29. Muzakkar, M. Z., Nurdin, M., Ismail, I., Maulidiyah, M., Wibowo, D., Ratna, R., Saad, S. K. M., & Umar, A. A. (2019). TiO_2 coated-asphalt buton photocatalyst for high-performance motor vehicles gas emission mitigation. *Emission Control Science and Technology*. https://doi.org/10.1007/s40825-019-00132-3
30. Nurdin, M., Prabowo, O. A., Arham, Z., Wibowo, D., Maulidiyah, M., Saad, S. K. M., & Umar, A. A. (2019). Highly sensitive fipronil pesticide detection on ilmenite (FeO.TiO2)-carbon paste composite electrode. *Surfaces and Interfaces, 16*, 108–113. https://doi.org/10.1016/j.surfin.2019.05.008
31. Azis, T., Nurwahidah, A. T., Wibowo, D., & Nurdin, M. (2017). Photoelectrocatalyst of Fe co-doped N-TiO2/Ti nanotubes: Pesticide degradation of thiamethoxam under UV–visible lights. *Environmental nanotechnology, monitoring & management, 8*, 103–111.
32. Nurdin, M., Ramadhan, L. O. A. N., Darmawati, D., Maulidiyah, M., & Wibowo, D. (2018). Synthesis of Ni, N co-doped TiO_2 using microwave-assisted method for sodium lauryl sulfate degradation by photocatalyst. *Journal of Coatings Technology and Research, 15*, 395–402. https://doi.org/10.1007/s11998-017-9976-8
33. Elysabeth, T., Agriyfani, D. A., Ibadurrohman, M., & Nurdin, M. (2020). Synthesis of Ni-and N-doped titania nanotube arrays for photocatalytic hydrogen production from glycerol–water solutions. *Catalysts, 10*, 1234.
34. Natsir, M., Putri, Y. I., Wibowo, D., Maulidiyah, M., Salim, L. O. A., Azis, T., Bijang, C. M., Mustapa, F., Irwan, I., & Arham, Z. (2021). Effects of Ni–TiO_2 pillared Clay–Montmorillonite composites for photocatalytic enhancement against reactive orange under visible light. *Journal of Inorganic and Organometallic Polymers and Materials, 31*, 3378–3388.
35. Tu, B., Chen, H., Deng, J., Xue, S., Ma, X., Xu, Y., Xie, Z., & Tao, H. (2021). Preparation of NI co-doped TiO2 supported on activated carbon photocatalyst for efficient photocatalytic reduction of Cr (VI) ions. *Colloids and Surfaces A: Physicochemical and Engineering Aspects, 622*, 126660.
36. Gabal, M. A. E.-F., Al Angari, Y. M., & Obaid, A. Y. (2013). Structural characterization and activation energy of NiTiO3 nanopowders prepared by the co-precipitation and impregnation with calcinations. *Comptes Rendus Chimie, 16*, 704–711.
37. Singh, V., Rao, A., Tiwari, A., Yashwanth, P., Lal, M., Dubey, U., Aich, S., & Roy, B. (2019). Study on the effects of Cl and F doping in TiO2 powder synthesized by a sol-gel route for biomedical applications. *Journal of Physics and Chemistry of Solids, 134*, 262–272.
38. Madima, N., Kefeni, K. K., Mishra, S. B., Mishra, A. K., & Kuvarega, A. T. (2022). Fabrication of magnetic recoverable Fe3O4/TiO2 heterostructure for photocatalytic degradation of rhodamine B dye. *Inorganic Chemistry Communications, 145*, 109966.
39. Abd, A. N., Ali, R. S., & Hussein, A. A. (2016). Fabrication and characterization of heterojunction nickel oxide nanoparticles/silicon. *Journal of Multidisciplinary Engineering Science Studies, 2*.
40. Guo, H., Wang, Y., Yao, X., Zhang, Y., Li, Z., Pan, S., Han, J., Xu, L., Qiao, W., & Li, J. (2021). A comprehensive insight into plasma-catalytic removal of antibiotic oxytetracycline based on graphene-TiO2-Fe3O4 nanocomposites. *Chemical Engineering Journal, 425*, 130614.
41. Munir, M., Ahmad, M., Saeed, M., Waseem, A., Nizami, A.-S., Sultana, S., Zafar, M., Rehan, M., Srinivasan, G. R., & Ali, A. M. (2021). Biodiesel production from novel non-edible caper (Capparis spinosa L.) seeds oil employing Cu–Ni doped ZrO2 catalyst, Renew. *Renewable and Sustainable Energy Reviews, 138*, 110558.

42. Nurdin, M., Fatma, F., Natsir, M., & Wibowo, D. (2017). Characterization of methyl ester compound of biodiesel from industrial liquid waste of crude palm oil processing. *Analytical chemistry research, 12*, 1–9.
43. Alsharifi, M., Znad, H., Hena, S., & Ang, M. (2017). Biodiesel production from canola oil using novel Li/TiO2 as a heterogeneous catalyst prepared via impregnation method. *Renewable Energy, 114*, 1077–1089.
44. Hossain, M. N., Siddik Bhuyan, M. S. U., Alam, A. H. M. A., & Seo, Y. C. (2019). Optimization of biodiesel production from waste cooking oil using S–TiO2/SBA-15 heterogeneous acid catalyst. *Catalysts, 9*, 67.
45. De, A., & Boxi, S. S. (2020). Application of Cu impregnated TiO2 as a heterogeneous nanocatalyst for the production of biodiesel from palm oil. *Fuel, 265*, 117019.
46. Soltani, S., Khanian, N., Choong, T. S. Y., Asim, N., & Zhao, Y. (2021). Microwave-assisted hydrothermal synthesis of sulfonated TiO2-GO core–shell solid spheres as heterogeneous esterification mesoporous catalyst for biodiesel production. *Energy Conversion and Management, 238*, 114165.